Inorganic Chemistry
Cite This: Inorg. Chem. XXXX, XXX, XXX−XXX
Article
pubs.acs.org/IC

Organometallic Ir(III) Phosphors Decorated by Carbazole/Diphenylphosphoryl Units for Efficient Solution-Processable OLEDs with Low Efficiency Roll-Offs

Wei-Lin Song,[†,⊥] Hui-Ting Mao,[†,⊥] Guo-Gang Shan,[*,†] Ying Gao,[†] Gang Cheng,[*,‡,§] and Zhong-Min Su[*,†,∥]

[†]Institute of Functional Material Chemistry and National & Local United Engineering Lab for Power Battery, Faculty of Chemistry, Northeast Normal University, Changchun, Jilin 130024, People's Republic of China

[‡]State Key Laboratory of Synthetic Chemistry, HKU-CAS, Joint Laboratory on New Materials, and Department of Chemistry, The University of Hong Kong, Pokfulam Road, Hong Kong SAR, People's Republic of China

[§]HKU Shenzhen Institute of Research and Innovation, Shenzhen 518053, People's Republic of China

[∥]Changchun University of Science and Technology, Changchun, Jilin 130022, People's Republic of China

Supporting Information

ABSTRACT: Recently, solution-processable PhOLEDs have been attracting great interest for their low cost and high productivity relative to the vacuum-deposited devices. Similar to vacuum-deposited OLEDs, however, they usually suffer from serious efficiency roll-offs, especially in high brightness. Finding a feasible way and/or designing novel materials to increase efficiencies and reduce roll-offs simultaneously are highly desired. Herein, a new family of solution-processable cyclometalated iridium(III) phosphors with carbazole (**Cz**) and/or diphenylphosphoryl (**Ph_2PO**) units functionalized main ligands has been designed. Owing to **Cz** and **Ph_2PO** moieties possessing bulky steric effects, they can suppress the intermolecular strong packing and then decrease TTA effects and emission quenching. Meanwhile, the resulting OLEDs based on the designed phosphors exhibit considerable efficiencies and relatively small efficiency roll-offs. The device based on **4** containing both **Cz** and **Ph_2PO** units realized a maximum current efficiency of 21.3 cd A^{-1}, accompanied by a small roll-off. By optimization of the configuration of OLEDs, the device performance can be further enhanced, demonstrating their potential for high-performance solution-processable PhOLEDs.

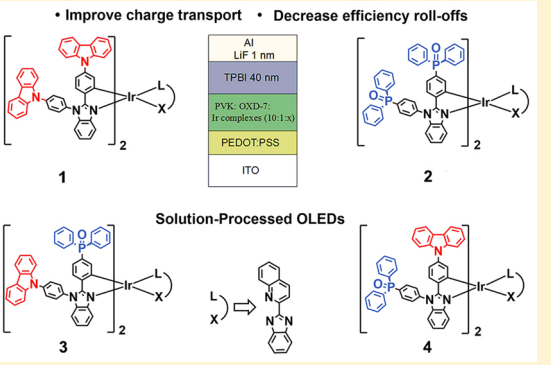

INTRODUCTION

As time goes on, more electrical energy is largely consumed to meet the needs of people's lives in lighting, luminaire, displays, and so on. It is thus obligatory to develop high-performance energy-conserving lighting devices. Owing to the superiorities of low energy consumption, wide viewing angle, and flexible display, organic light-emitting diodes (OLEDs) have been applied in displays and energy-saving lighting.[1−4] Phosphorescent transition-metal materials possess strong spin−orbit coupling and fast intersystem crossing rates, and they can utilize almost 100% of the excitons to realize high electroluminescence (EL) efficiencies.[5−7] Among the phosphorescent materials, iridium(III) phosphors have drawn much attention on account of the high emission efficiencies, excellent photothermal stability, and tunable emission color.[7−12] Some representative works on iridium(III)-based OLEDs have been summarized in recent reviews.[13−16]

To date, two main processing techniques are used to fabricate the OLEDs: the first is a vacuum-deposition process, and the second is a spin-coating solution process.[17] Although the OLEDs can achieve high performance, serious efficiency roll-offs still exist for a long time during the device operation, which hinder their widespread use in practical applications.[18,19] In addition, the vacuum deposition process requires intricate technological means and throws away a large amount of organic materials. Furthermore, it is also highly expensive to maintain the chamber under vacuum, leading to expensive fabrication costs. Alternatively, a more low-cost method, i.e., a solution-processable technique, has been developed recently.[20−22] Therefore, it is important to design novel iridium(III) phosphors or develop new strategies to optimize the device performances.

Many groups have devoted great efforts to the development of a variety of iridium(III) phosphors to fabricate PhOLEDs with low efficiency roll-offs.[23−26] One of the effective ways to

Received: May 29, 2019

DOI: 10.1021/acs.inorgchem.9b01601
Inorg. Chem. XXXX, XXX, XXX−XXX

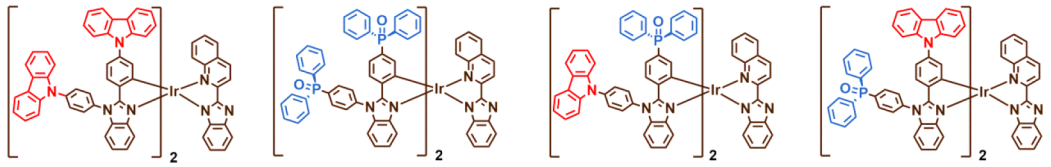

1 2 3 4

Figure 1. Chemical structures of **1**−**4**.

Table 1. Photophysical and Electrochemical Data of 1−4

phosphor	λ_{abs}[a] (nm)	$\lambda_{PL,max}$[a−c] (nm)	Φ_p[a,c] (%)	τ[a,c] (μs)	E_g[d] (eV)	$E_{ox,onset}$[e] (V)	HOMO[f] (eV)	LUMO[g] (eV)
1	292	581, 555, 582	25.2, 10.1	1.32, 0.48	2.18	0.39	−5.19	−3.01
	338							
	412							
2	298	565, 553, 579	29.7, 24.3	1.09, 0.70	2.24	0.38	−5.18	−2.94
	368							
	409							
3	292	569, 555, 577	32.1, 16.1	1.24, 0.61	2.23	0.41	−5.21	−2.98
	365							
	403							
4	292	577, 557, 581	27.1, 17.4	1.24, 0.74	2.23	0.41	−5.21	−2.98
	354							
	413							

[a]Measured in dichloromethane solution at 298 K. [b]Measured in dichloromethane solution at 77 K. [c]Spin-coated thin film. [d]Optical band gap. [e]The onset oxidation potential. [f]Calculated from the onset oxidation potentials of the complexes. [g]Calculated using the equation $E_{LUMO} = E_{HOMO} + E_g$.

achieve high-performance solution-processable OLEDs is designing dendrimers,[27,28] which possess good processability to ensure the formation of homogeneous thin films. In addition, such a strategy can suppress self-quenching to improve the efficiency and weaken the efficiency roll-offs simultaneously. In 2017, Ding and co-workers synthesized red iridium(III) dendrons containing oligocarbazole and doped devices with a current efficiency (CE) of 25.7 cd A^{-1} were realized, whose CE still remained as high as 23.9 cd A^{-1} at a brightness of 1000 cd m^{-2}.[29] Although such a strategy is effective, the synthetic procedures require cumbersome steps with relatively low total yields. Recent works have shown that attaching appropriate functional groups with intrinsic electron-/hole-transporting characteristics can effectively adjust the carrier-transporting properties and improve the corresponding device performances.[27,30−33]

Recently, many cyclometalated iridium(III) phosphors based on the 1,2-diphenyl-*H*-benzimidazole (**HPBI**) moiety as the main ligand have been reported.[34−36] Various iridium(III) phosphors with carbazole (**Cz**)- or diphenylphosphoryl (**Ph_2PO**)-functionalized **HPBI** ligands have been designed. The resulting vacuum-deposited OLEDs exhibit high EL performances due to the steric hindrance effect of **Cz** and **Ph_2PO** that can effectively weaken self-quenching and control charge-carrier characters as well.[37] To determine whether such molecular structures were suitable for constructing iridium(III) phosphors for solution-processable devices, herein, we successfully synthesized a new family of iridium(III) phosphors, denoted **1**−**4**, in which the **HPBI** ligand was functionalized with **Cz** and **Ph_2PO** moieties (see Figure 1). Meanwhile, we employed 2-benzo[*d*]imidazol-2-ylquinoline (**Hbiq**) as an ancillary ligand to achieve long-wavelength emissions. High-performance solution-processable devices employing the designed iridium(III) phosphors as emissive layers have been achieved with considerable efficiencies and relatively low roll-offs. By manipulation of the doping concentration of luminescent materials, the device based on **4** exhibited eminent performance, displaying a maximum CE of 21.3 cd A^{-1} and low efficiency roll-off of 11.2%. The EL performances for such devices, in fact, could be further optimized by changing the device structure.

EXPERIMENTAL SECTION

General Information. The experimental details and synthetic routes for the cyclometalated and ancillary ligands as well as the studied complexes can be found in the Supporting Information. Briefly, modified procedures were used to synthesize all cyclometalated ligands in relatively high yield,[37] and the ancillary ligand **Hbiq** used was prepared in accordance with a previous work.[38] The target complexes **1**−**4** were then obtained by reacting the corrsponding μ-chloro-bridged dimer with the **Hbiq** ligand. All complexes were characterized by various spectroscopic techniques (see the Supporting Information).

Physical Measurements. The photophysical characteristics of **1**−**4** in CH_2Cl_2 solution with a concentration of 1.0×10^{-5} M were detected. Cary 500 UV−vis−NIR and FL-4600 fluorescent spectrophotometers were used to measure their absorption spectra and photoluminescence (PL) spectra, respectively. Meanwhile, the corresponding films for phosphors were acquired via a spin-coating method with a concentration of 20 mg mL^{-1} in CH_2Cl_2. In addition, the excited-state lifetimes and photoluminescence quantum yields (PLQYs) were monitored by an Edinburgh FLSP920 spectrofluorimeter and an integrating sphere.

Theoretical Calculations. The Gaussian 09 program package was used to calculate the studied phosphors.[39] The closed-shell and spin-unrestricted open-shell B3LYP methods under gas-phase conditions were carried out to optimize the geometries in both the ground state and the lowest triplet state (T_1), respectively.[40] The LANL2DZ basis set was used for the Ir atom, and the standard 6-31G* set was employed for the rest of the atoms. The inner-core electrons located on the central Ir(III) atom were replaced by effective core potentials, and the outer-core electrons $(5s)^2(5p)^6$ and valence electrons $(5d)^6$ were left to study.[41] TD-DFT calculations were then performed using the CPCM polarizable conductor calculation model (dichloro-

DOI: 10.1021/acs.inorgchem.9b01601
Inorg. Chem. XXXX, XXX, XXX−XXX

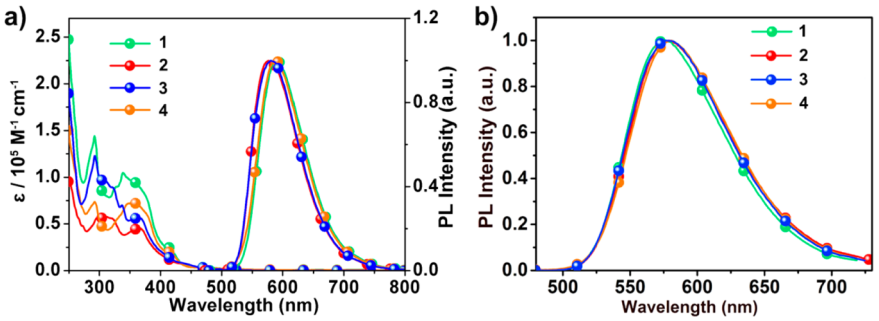

Figure 2. (a) Absorption and emission spectra of **1**−**4** in dichloromethane (10^{-5} M) at room temperature. (b) Emission spectra of those phosphors in neat films.

methane solvent) at the optimized geometry to deeply understand the excited-state characteristics.

Electrochemical Measurements. Cyclic voltammetry (CV) measurements for all phosphors with a concentration of 0.003 M in CH_2Cl_2 were carried out using an electrochemical workstation (BAS100W instrument), in which ferrocene was used as the internal standard. An aqueous saturated calomel electrode, a platinum-wire electrode, and a glassy-carbon electrode were selected as the reference electrode, the auxiliary electrode, and the working electrode, respectively. Tetrabutylammonium hexafluorophosphate (1×10^{-1} M) was used as the supporting electrolyte.

Device Fabrication and Characterization. The devices were fabricated on patterned indium−tin oxide (ITO) coated glass substrates with a sheet resistance of 30 Ω/sqr. All glass substrates were cleaned with Decon 90 and rinsed with deionized water. Then, they were dried in an oven, following a treatment in an ultraviolet−ozone chamber. PEDOT:PSS was spin-coated onto the glass substrates as the hole-transporting layer. Then, a mixture of the iridium(III) complex with PVK and OXD-7 was prepared as a 10 mg cm^{-3} solution in dichloromethane and spin-coated onto the PEDOT:PSS layer to form the emissive layer. Next, TPBI was selected as the electron-transporting layer. Finally, LiF/Al was vacuum-deposited as the metal cathode. An Ocean Optics Maya 2000-PRO spectrometer, Minolta LS-110 luminance meter, and Keithley 2400 source meter were used to test the EL spectra and luminance efficiency−voltage characteristics of the resulting devices.

RESULTS AND DISCUSSION

Photophysical Properties. UV−vis absorption and PL spectra of **1**−**4** were recorded in CH_2Cl_2 at room temperature, and the numerical data are summarized in Table 1. As for most iridium(III) phosphors, the absorptions below 380 nm are assigned to allowed $^1\pi-\pi^*$ transitions in the center of the ligands, as shown in Figure 2a. Weak and broad absorptions are found at a longer wavelength (>400 nm) due to ^{1}MLCT (metal to ligand charge transition), ^{3}MLCT, and $^3\pi-\pi^*$ transitions.[8,42] To better comprehend the features of the excited states involved in the main transitions, we simulated the absorption spectra by performing TDDFT calculations (see Tables S1−S4 and Figures S1−S4). With complex **4** as an example, the absorption bands below 380 nm from the excitation of S_4, S_{16}, and S_{19} are mainly ascribed to $\pi-\pi^*$ transitions of both the main ligands and ancillary ligands. The long absorption bands have obvious ^{1}MLCT characters. The calculated UV−vis absorption spectra matched well with the experimental spectra. The corresponding assignments for complexes **1**−**3** can be also obtained from the TD-DFT results.

Upon photoexcitation, **1** and **4** exhibit identical emission maxima of 581 and 577 nm, respectively, accompanied by Φ = 25.2% (**1**) and Φ = 27.1% (**4**). In addition, **2** and **3** exhibit strong emission with peaks of 565 and 569 nm as well as Φ = 29.7% (**2**) and Φ = 32.1% (**3**), respectively. Moreover, the emission spectra of **1**−**4** at 77 K WERE tested in dichloromethane with peak maximA of 555, 553, 555, and 557 nm, respectively (see Figure S5). The hypochromatic shift observed relative to the emission at room temperature indicates that the PL spectra for all phosphors are sensitive to temperature.[43] Therefore, it is shown that the emissions of the phosphors should be of mixed ^{3}MLCT, ^{3}LLCT, or ^{3}ILCT character.[44−48]

To explore the emission character of all phosphors, the lifetimes were tested in both solutions and thin films. They exhibit a microsecond excited-state decay, which obviously reveals the phosphorescence emission character.[46,49,50] Additionally, the spin-coated neat films PL spectra based on **1**−**4** had a negligible red shift compared to those in solution, probably due to the effective medium polarity in films (see Table1). It is worth noting that, although different functional groups have been introduced into the phosphors, they exhibit almost identical emissions in spin-coated films. This result indicates that the peripheral **Cz** and **Ph_2PO** units have a slight effect on their emission in films but can adjust the charge-transporting characteristics and the solid-state packing as well. Therefore, we conjecture that devices based on these materials would exhibit similar EL emission profiles but distinct different EL performances caused by their different charge-transporting properties and intermolecular interactions in the films.

Theoretical Calculations. To deepen the understanding of the influence of functional groups on the photophysical and electrochemical properties for all phosphors, the corresponding theoretical calculations were implemented. The highest occupied molecular orbital (HOMO) and the lowest unoccupied molecular orbital (LUMO) with corresponding energy levels are displayed in Figure 3. The LUMOs for **1**−**4** are mainly distributed on the ancillary ligand. The HOMOs of all complexes are mainly composed of a mixture of the d orbitals for the Ir(III) atoms and some distributions on the ancillary ligands. The T_1 states of **1**−**4** originate from HOMO → LUMO (73%), HOMO → LUMO (89%), HOMO → LUMO (70%), HOMO → LUMO (90%) transitions, respectively (see Table S5,). Therefore, it is speculated that all phosphors should possess ^{3}MLCT/^{3}ILCT character in different proportions. Spin densities calculated by unrestricted DFT methods are more localized on iridium(III) atoms as well as on the ancillary ligands, which matches well with the topology of the HOMO → LUMO excitations for these complexes (see Figure S6 in the Supporting Information). These results are consistent with the observed phosphorescent emission profiles are both room temperature and 77 K. In addition, according to triplet excited state calculations obtained

DOI: 10.1021/acs.inorgchem.9b01601
Inorg. Chem. XXXX, XXX, XXX−XXX

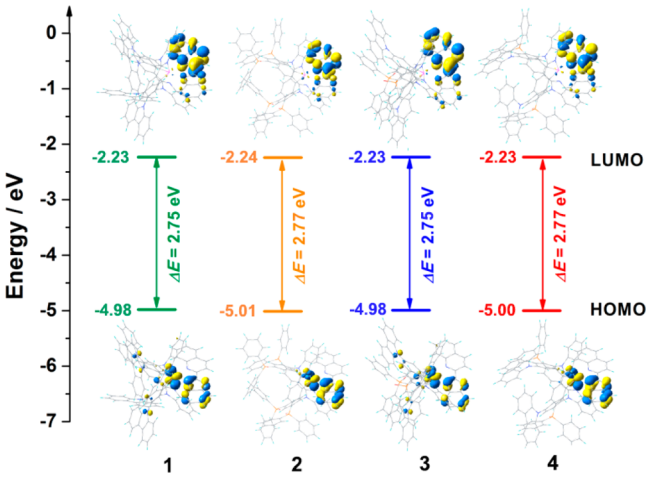

Figure 3. HOMO and LUMO distributions of **1**−**4**.

by TD-DFT, their excited state characters were further confirmed by electron density difference analysis (see Figure S7 in the Supporting Information).

Electrochemical Properties. As shown in Figure S8 and Table 1, the electrochemical behaviors of Ir(III) phosphors were studied. The E_{HOMO} values are evaluated to be −5.19, −5.18, −5.21, and −5.21 eV for **1**−**4**, respectively, from the onset oxidation potentials in CV curves. On the basis of E_{HOMO} and optical band gaps (E_g), the E_{LUMO} values of **1**−**4** are calculated to be −3.01, −2.94, −2.98, and −2.98 eV (see Figure S8 in the Supporting Information).[51,52]

Device Performance. Taking into full consideration of the good solubility of the iridium(III) phosphors, we fabricated solution-processable devices with the configuration of ITO/PEDOT:PSS/PVK:OXD-7:iridium(III) phosphors (10:1:*x*)/TPBI (40 nm)/LiF (1.2 nm)/Al (100 nm) (see Figure 4a). The HOMO/LUMO diagrams and molecular structures of used materials in the devices are displayed in Figure 5. Here, ITO and LiF/Al were employed as the anode and cathode, respectively, poly(3,4-ethylene-dioxythiophene)-poly(styrenesulfonate) (PEDOT:PSS) acted as the hole-injecting layer (HIL), and 1,3,5-tris(1-phenyl-1*H*-benzimidazol-2-yl)-benzene (TPBI) was chosen as the electron-transporting layer. The emissive layer was prepared by spin-coating a solution of a poly(*N*-vinylcarbazole) (PVK):2,2′-(1,3-phenylene)bis[5-(4-*tert*-butylphenyl)-1,3,4-oxadiazole] (OXD-7):iridium(III) blend at different concentrations. Figure 4c−f displays the normalized EL spectra of the solution-processable OLEDs based on **1**−**4**. The electroluminescent profiles of the devices are almost similar to their emission spectra, which indicate that the electroluminescence and photoluminescence should

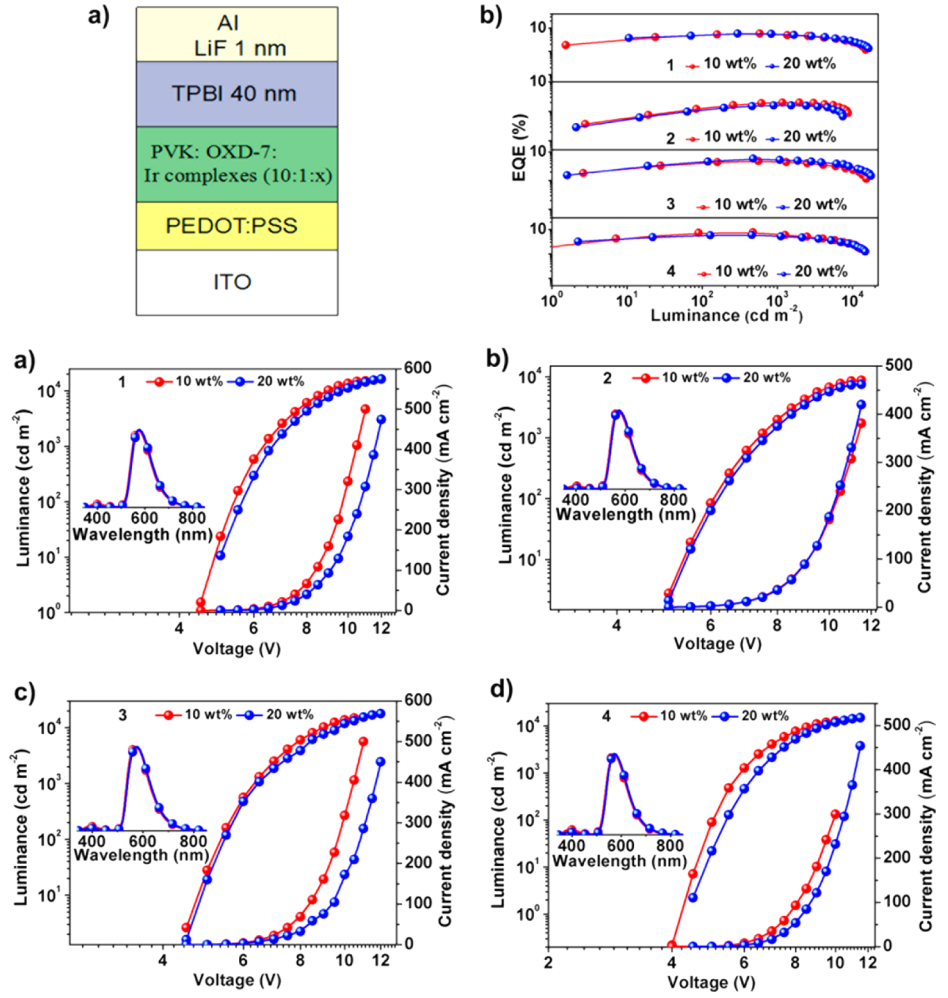

Figure 4. (a) The OLED device structure. (b) EQE curves of all devices. EL spectra (inset) and *J*−*V*−*L* characteristics of devices based on **1** (c), **2** (d), **3** (e), and **4** (f).

DOI: 10.1021/acs.inorgchem.9b01601
Inorg. Chem. XXXX, XXX, XXX−XXX

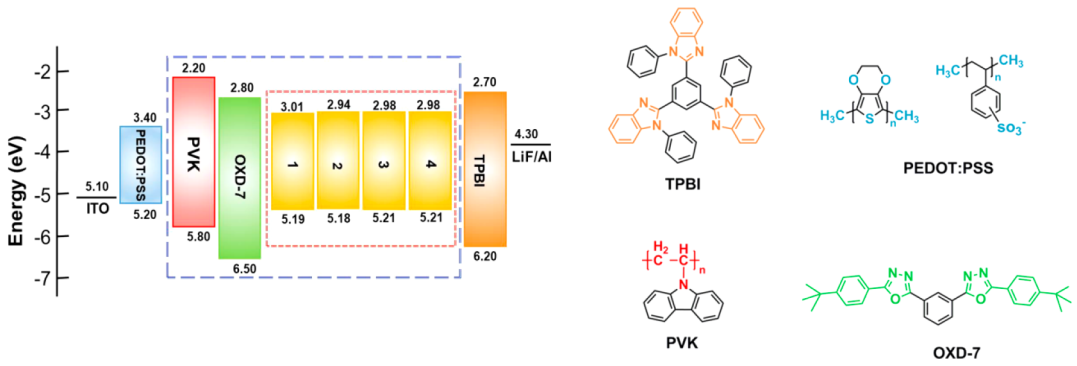

Figure 5. Energy level diagram of doped devices and the chemical structures of employed materials.

Table 2. Summary of EL Performances of Studied Devices

			CE (cd A^{-1})[b] (CE roll-off (%))		PE (lm W^{-1})[c] (PE roll-off (%))		EQE (%)[d] (EQE roll-off (%))		
device	doping concn (wt %)	L (cd m^{-2})[a]	max	at 1000 cd m^{-2}	max	at 1000 cd m^{-2}	max	at 1000 cd m^{-2}	CIE (x, y)
1	10	15200	15.8	14.7 (6.9)	8.4	7.7 (8.3)	5.8	5.3 (8.6)	(0.50, 0.49)
	20	16400	15.6	14.7 (5.8)	8.2	6.9 (15.8)	5.8	5.5 (5.2)	(0.51, 0.49)
2	10	8750	5.5	5.5 (0.0)	2.4	2.3 (2.5)	2.0	2.0 (0.0)	(0.48, 0.50)
	20	7470	4.4	4.3 (2.3)	1.8	1.7 (4.1)	1.6	1.6 (0.0)	(0.50, 0.49)
3	10	15400	13.5	12.8 (4.9)	7.1	6.5 (8.4)	4.8	4.5 (6.2)	(0.49, 0.50)
	20	17880	15.9	14.3 (9.4)	8.3	7.0 (15.6)	6.8	5.3 (22.1)	(0.50, 0.49)
4	10	12800	21.3	18.9 (11.2)	12.8	9.9 (22.6)	7.6	6.6 (13.1)	(0.49, 0.50)
	20	14850	16.2	14.5 (10.5)	9.0	7.1 (21.1)	5.9	5.3 (10.1)	(0.50, 0.49)
2[e]	10	11140	13.7	12.2 (10.9)	6.6	5.1 (22.7)	4.8	4.3 (10.4)	(0.48, 0.49)

[a]Maximum luminance of the devices. [b]The maximum CE and the values measured at 1000 cd m^{-2} at different concentrations. [c]The maximum PE and the values measured at 1000 cd m^{-2} at different concentrations. [d]The maximum EQE and the values measured at 1000 cd m^{-2} at different concentrations. [e]The device configuration ITO/PEDOT:PSS/PVK:**2** (10:1:x)/TPBI (40 nm)/LiF (1.2 nm)/Al (100 nm).

originate from the decay of the same excitons and without any unfavorable excimeric emission. What is more, the photoluminescence spectra of doped films show absolute energy transfer between the host and guest materials (see Figures S9–S11 in the Supporting Information). In addition, the luminescence quantum yields of all phosphors doped in the PVK and OXD-7 thin films were also measured. All of the doped films exhibit relatively high PLQYs, and the corresponding data are given in Table S6. It is clear that the **4**-based doped film with a doping concentration of 10 wt % exhibits the best PLQY, as high as 65.1%, showing good energy transfer from the host to guest as well as weak emission quenching in the doping film. Therefore, we speculate the device employing **4** as emitting layer would show better EL performances.

The phosphors **1**–**4** were individually doped into PVK and OXD-7 at different concentrations of 10 and 20 wt %, respectively. Figure 4b–f shows the external quantum efficiency (EQE) and current density–voltage–luminance (J–V–L) characteristics of EL devices. Bright yellow electroluminescence can be recorded with Commission Internationale de l'Éclairage (CIE) coordinates of (0.50, 0.49) (10 wt %) and (0.51, 0.49) (20 wt %) for **1**, (0.48, 0.50) (10 wt %) and (0.50, 0.49) (20 wt %) for **2**, (0.49, 0.50) (10 wt %) and (0.50, 0.49) (20 wt %) for **3**, and (0.49, 0.50) (10 wt %) and (0.50, 0.49) (20 wt %) for **4**. The CIE coordinates of the devices are almost consistent at different doping concentrations, which are extraordinarily important for the precise control of the emission energies of the iridium(III) phosphors via modifying cyclometalated ligands as well as the color purity of the OLEDs.[53]

As shown in Figure 4c–f, the devices achieve favorable luminance; for example, the maximum brightnesses (L_{max}) of **3**-based devices are as high as 15400 cd m^{-2} (10 wt %) and 17880 cd m^{-2} (20 wt %). The maximum brightnesses (L_{max}) of **4**-based devices are 12800 cd m^{-2} (10 wt %) and 14850 cd m^{-2} (20 wt %). Table 2 reveals the device performances. **3** and **4** endow their devices with promising efficiencies, with maximum CEs of 13.5 cd A^{-1} (10 wt %) and 15.9 cd A^{-1} (20 wt %) and and 21.3 cd A^{-1} (10 wt %) and 16.2 cd A^{-1} (20 wt %), respectively. Significantly, they all exhibit low efficiency roll-offs. At 1000 cd m^{-2}, the current efficiencies for **3**- and **4**-based devices are slightly decreased to 12.8 and 18.9 cd A^{-1} at a doping concentration of 10 wt %, corresponding to efficiency roll-offs of only 4.9% and 11.2%, respectively. As expected, the **4**-based doped OLED displays excellent performance, showing the highest efficiency among all studied devices, which is probably due to its higher PLQY in doped film as mentioned above and better charge carrier balance in the device. The **Ph_2PO/Cz** groups introduced into the complex can effectively reduce the intermolecular aggregation and suppress self-quenching effects, leading to the favorable stability of EL efficiency. Moreover, the more balanced carrier transport characteristic probably enlarges the recombination zone and efficiently confines the triplet excitons generated within the EML.[54,55] In general, it is believed that carbazole and diphenylphosphoryl groups could increase the overall device efficiency and decrease the efficiency roll-offs to a certain degree.

DOI: 10.1021/acs.inorgchem.9b01601
Inorg. Chem. XXXX, XXX, XXX–XXX

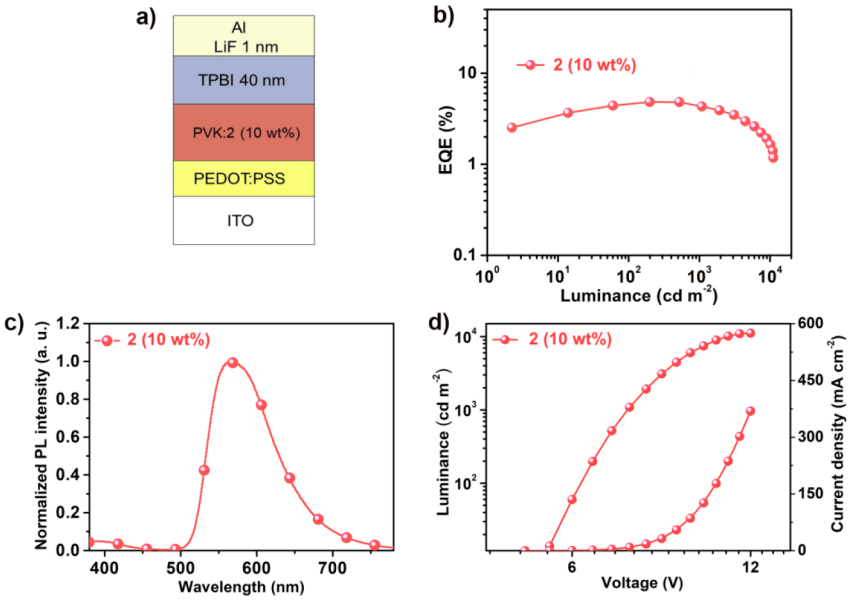

Figure 6. (a) Optimized device configuration for **2**. (b) EQE curves of the device. (c) EL spectra of the device. (d) Current density−voltage−luminance characteristics.

As can be seen in Figure 4d and Table 2, the efficiencies of the devices based on **2** are much lower than those of its counterparts having the same device structure of ITO/PEDOT:PSS/PVK:OXD-7:iridium(III) phosphors (10:1:*x*)/TPBI (40 nm)/LiF (1.2 nm)/Al (100 nm). The phenomenon may be ascribed to the introduction of two **Ph_2PO** units into the cyclometalated ligands, leading to imbalanced charge carriers in the EML. To further optimize the device performance, we removed the electron-transporting material OXD-7 in the EML for **2**-based devices with the aim of manipulating charge-carrier transportation. The corresponding device configuration and is displayed in Figure 6a. By optimization, the maximum CE reaches 13.7 cd A^{-1}, which is an increase of about 3-fold over the previous data. In addition, the optimized device also exhibits a low efficiency roll-off of only 10.9% for CE at 1000 cd m^{-2} (see Figure 6b−d and Table 2).

CONCLUSIONS

In general, a new family of iridium(III) phosphors named **1**−**4** were designed and synthesized, in which the cyclometalated ligands were substituted by **Cz** and/or **Ph_2PO** groups simultaneously. The intermolecular interaction and emission quenching could be suppressed to some extent, due to the strong steric effects caused by the **Cz** and **Ph_2PO** units. Meanwhile, the charge-carrier transporting characters of the complexes were well manipulated by controlling the number and position of such large functional groups. Therefore, the corresponding phosphors displayed low efficiency roll-offs even when the doping concentration was high. The doped device based on **4** displayed eminent performance with a CE of 21.3 cd A^{-1}. This work emphasizes the significance of large functional groups in optimizing cyclometalated iridium(III) phosphors used in solution-processable OLEDs. What is more, it provides a feasible strategy for the future development of iridium(III) phosphors and relevant optical devices.

ASSOCIATED CONTENT

Supporting Information

The Supporting Information is available free of charge on the ACS Publications website at DOI: 10.1021/acs.inorgchem.9b01601.

Supplemental schemes and photophysical and theoretical data of all complexes (PDF)

AUTHOR INFORMATION

Corresponding Authors

*Email for G.-G.S.: shangg187@nenu.edu.cn.
*Email for G.C.: ggcheng@hku.hk.
*Email for Z.-M.S.: zmsu@nenu.edu.cn.

ORCID

Gang Cheng: 0000-0001-8081-8205
Zhong-Min Su: 0000-0002-3342-1966

Author Contributions

⊥W.-L.S. and H.-T.M. contributed equally to this work.

Notes

The authors declare no competing financial interest.

ACKNOWLEDGMENTS

The authors gratefully acknowledge financial support from the National Natural Science Foundation of China (21303012, 21273030, 51203017, 21131001, and 61474054), the 973 Program (2013CB834801), the fundamental Research Funds for the Central Universities (2412019FZ012 and 2412019QD007), the Basic Research Program of Shenzhen (JCYJ20170818141858021), and the Telecommunications Scientific Foundation (NY215061).

REFERENCES

(1) Tang, C. W.; VanSlyke, S. A. Organic electroluminescent diodes. *Appl. Phys. Lett.* **1987**, *51*, 913−915.
(2) Suwanprateeb, J. Improvement in mechanical properties of three-dimensional printing parts made from natural polymers reinforced by acrylate resin for biomedical applications: a double infiltration approach. *Polym. Int.* **2006**, *55*, 57−62.

DOI: 10.1021/acs.inorgchem.9b01601
Inorg. Chem. XXXX, XXX, XXX−XXX

(3) Huang, J.; Nie, H.; Zeng, J.; Zhuang, Z.; Gan, S.; Cai, Y.; Guo, J.; Su, S. J.; Zhao, Z.; Tang, B. Z. Highly Efficient Nondoped OLEDs with Negligible Efficiency Roll-Off Fabricated from Aggregation-Induced Delayed Fluorescence Luminogens. *Angew. Chem., Int. Ed.* **2017**, *56*, 12971−12976.
(4) Li, X.; Zhang, J.; Zhao, Z.; Wang, L.; Yang, H.; Chang, Q.; Jiang, N.; Liu, Z.; Bian, Z.; Liu, W.; Lu, Z.; Huang, C. Deep Blue Phosphorescent Organic Light-Emitting Diodes with CIEy Value of 0.11 and External Quantum Efficiency up to 22.5%. *Adv. Mater.* **2018**, *30*, 1705005.
(5) Reineke, S.; Lindner, F.; Schwartz, G.; Seidler, N.; Walzer, K.; Lüssem, B.; Leo, K. White organic light-emitting diodes with fluorescent tube efficiency. *Nature* **2009**, *459*, 234−238.
(6) Baldo, M. A.; O'Brien, D. F.; You, Y.; Shoustikov, A.; Sibley, S.; Thompson, M. E.; Forrest, S. R. Highly efficient phosphorescent emission from organic electroluminescent devices. *Nature* **1998**, *395*, 151−154.
(7) Fan, C.; Li, Y.; Yang, C.; Wu, H.; Qin, J.; Cao, Y. Phosphoryl/Sulfonyl-Substituted Iridium Complexes as Blue Phosphorescent Emitters for Single-Layer Blue and White Organic Light-Emitting Diodes by Solution Process. *Chem. Mater.* **2012**, *24*, 4581−4587.
(8) Lamansky, S.; Djurovich, P.; Murphy, D.; Feras, A. R.; Lee, H. E.; Adachi, C.; Paul, E. B.; Forrest, S. R.; Thompson, M. E. Highly Phosphorescent Bis-Cyclometalated Iridium Complexes: Synthesis, Photophysical Characterization, and Use in Organic Light Emitting Diodes. *J. Am. Chem. Soc.* **2001**, *123*, 4304−4312.
(9) Ding, J.; Wang, B.; Yue, Z.; Yao, B.; Xie, Z.; Cheng, Y.; Wang, L.; Jing, X.; Wang, F. Bifunctional green iridium dendrimers with a "self-host" feature for highly efficient nondopedelectrophosphorescent devices. *Angew. Chem., Int. Ed.* **2009**, *48*, 6664−6666.
(10) You, Y.; Nam, W. Photofunctional triplet excited states of cyclometalatedIr(III) complexes: beyond electroluminescence. *Chem. Soc. Rev.* **2012**, *41*, 7061−7084.
(11) Adachi, C.; Baldo, M. A.; Thompson, M. E.; Forrest, S. R. Nearly 100% internal phosphorescence efficiency in an organic light-emitting device. *J. Appl. Phys.* **2001**, *90*, 5048−5051.
(12) Lin, J.; Wang, Y.; Gnanasekaran, P.; Chiang, Y.-C.; Yang, C.-C.; Chang, C.-H.; Liu, S.-H.; Lee, G.-H.; Chou, P.-T.; Chi, Y.; Liu, S.-W. Unprecedented Homoleptic Bis-Tridentate Iridium(III) Phosphors: Facile, Scaled-Up Production, and Superior Chemical Stability. *Adv. Funct. Mater.* **2017**, *27*, 1702856.
(13) Yang, X.; Zhou, G.; Wong, W. Y. Functionalization of phosphorescent emitters and their host materials by main-group elements for phosphorescent organic light-emitting devices. *Chem. Soc. Rev.* **2015**, *44*, 8484−8575.
(14) Wong, W.-Y.; Ho, C.-L. Functional metallophosphors for effective charge carrier injection/transport: new robust OLED materials with emerging applications. *J. Mater. Chem.* **2009**, *19*, 4457−4482.
(15) Ma, D.; Tsuboi, T.; Qiu, Y.; Duan, L. Recent Progress in Ionic Iridium(III) Complexes for Organic Electronic Devices. *Adv. Mater.* **2017**, *29*, 1603253.
(16) Song, W.; Lee, J. Y. Degradation Mechanism and Lifetime Improvement Strategy for Blue Phosphorescent Organic Light-Emitting Diodes. *Adv. Opt. Mater.* **2017**, *5*, 1600901.
(17) Shibata, M.; Sakai, Y.; Yokoyama, D. Advantages and disadvantages of vacuum-deposited and spin-coated amorphous organic semiconductor films for organic light-emitting diodes. *J. Mater. Chem. C* **2015**, *3*, 11178−11191.
(18) Baldo, M. A.; Adachi, C.; Forrest, S. R. Transient analysis of organic electrophosphorescence. II. Transient analysis of triplet-triplet annihilation. *Phys. Rev. B: Condens. Matter Mater. Phys.* **2000**, *62*, 10967.
(19) Giebink, N. C.; Forrest, S. R. Quantum efficiency roll-off at high brightness in fluorescent and phosphorescent organic light emitting diodes. *Phys. Rev. B: Condens. Matter Mater. Phys.* **2008**, *77*, 235215.
(20) Aizawa, N.; Pu, Y. J.; Chiba, T.; Kawata, S.; Sasabe, H.; Kido, J. Instant low-temperature cross-linking of poly(N-vinylcarbazole) for solution-processed multilayer blue phosphorescent organic light-emitting devices. *Adv. Mater.* **2014**, *26*, 7543−7546.
(21) Liu, C.; Fu, Q.; Zou, Y.; Yang, C.; Ma, D.; Qin, J. Low Turn-on Voltage, High-Power-Efficiency, Solution-Processed Deep-Blue Organic Light-Emitting Diodes Based on Starburst Oligofluorenes with Diphenylamine End-Capper to Enhance the HOMO Level. *Chem. Mater.* **2014**, *26*, 3074−3083.
(22) Wang, Z.; Lou, Y.; Naka, S.; Okada, H. Competitive emission process in mixed single layer top-emission organic light emitting device with reduced efficiency roll-off. *Appl. Phys. Lett.* **2010**, *97*, 203302.
(23) Cao, H. T.; Sun, H. Z.; Yin, Y. M.; Wen, X. M.; Shan, G. G.; Su, Z. M.; Zhong, R. L.; Xie, W. F.; Li, P.; Zhu, D. X. Iridium(iii) complexes adopting 1,2-diphenyl-1H-benzoimidazole ligands for highly efficient organic light-emitting diodes with low efficiency roll-off and non-doped feature. *J. Mater. Chem. C* **2014**, *2*, 2150−2159.
(24) Mao, H.-T.; Zang, C.-X.; Wen, L.-L.; Shan, G.-G.; Sun, H.-Z.; Xie, W.-F.; Su, Z. M. Ir(III) Phosphors Modified with Fluorine Atoms in Pyridine-1,2,4-triazolyl Ligands for Efficient OLEDs Possessing Low-Efficiency Roll-off. *Organometallics* **2016**, *35*, 3870−3877.
(25) Wen, L.-L.; Yu, J.; Sun, H.-Z.; Shan, G.-G.; Xie, W.-F.; Su, Z.-M. Low efficiency roll-off and high performance OLEDs employing alkyl group modified iridium(iii) complexes as emitters. *RSC Adv.* **2016**, *6*, 111556−111563.
(26) Han, C.; Xie, G.; Xu, H.; Zhang, Z.; Xie, L.; Zhao, Y.; Liu, S.; Huang, W. A single phosphine oxide host for high-efficiency white organic light-emitting diodes with extremely low operating voltages and reduced efficiency roll-off. *Adv. Mater.* **2011**, *23*, 2491−2496.
(27) Zhu, M.; Li, Y.; Miao, J.; Jiang, B.; Yang, C.; Wu, H.; Qin, J.; Cao, Y. Multifunctional homoleptic iridium(III) dendrimers towards solution-processed nondoped electrophosphorescence with low efficiency roll-off. *Org. Electron.* **2014**, *15*, 1598−1606.
(28) Ding, J.; Lü, J.; Cheng, Y.; Xie, Z.; Wang, L.; Jing, X.; Wang, F. Solution-Processible Red Iridium Dendrimers based on Oligocarbazole Host Dendrons: Synthesis, Properties, and their Applications in Organic Light-Emitting Diodes. *Adv. Funct. Mater.* **2008**, *18*, 2754−2762.
(29) Zhao, L.; Wang, S.; Lü, J.; Ding, J.; Wang, L. Solution processable red iridium dendrimers containing oligocarbazole dendrons for efficient nondoped and doped phosphorescent OLEDs. *J. Mater. Chem. C* **2017**, *5*, 9753−9760.
(30) Xu, H.; Chen, R.; Sun, Q.; Lai, W.; Su, Q.; Huang, W.; Liu, X. Recent progress in metal-organic complexes for optoelectronic applications. *Chem. Soc. Rev.* **2014**, *43*, 3259−3302.
(31) Yang, C. L.; Zhang, X. W.; You, H.; Zhu, L. Y.; Chen, L. Q.; Zhu, L. N.; Tao, Y. T.; Ma, D. G.; Shuai, Z. G.; Qin, J. G. Tuning the Energy Level and Photophysical and Electroluminescent Properties of Heavy Metal Complexes by Controlling the Ligation of the Metal with the Carbon of the Carbazole Unit. *Adv. Funct. Mater.* **2007**, *17*, 651−661.
(32) Zhou, G.; Ho, C.-L.; Wong, W.-Y.; Wang, Q.; Ma, D.; Wang, L.; Lin, Z.; Marder, T. B.; Beeby, A. Manipulating Charge-Transfer Character with Electron-Withdrawing Main-Group Moieties for the Color Tuning of Iridium Electrophosphors. *Adv. Funct. Mater.* **2008**, *18*, 499−511.
(33) Pu, Y.-J.; Iguchi, N.; Aizawa, N.; Sasabe, H.; Nakayama, K.-i.; Kido, J. fac-Tris(2-phenylpyridine)iridiums(III), covalently surrounded by six bulky host dendrons, for a highly efficient solution-processed organic light emitting device. *Org. Electron.* **2011**, *12*, 2103−2110.
(34) Shan, G. G.; Li, H. B.; Sun, H. Z.; Cao, H. T.; Zhu, D. X.; Su, Z. M. Enhancing the luminescence properties and stability of cationic iridium(III) complexes based on phenylbenzoimidazole ligand: a combined experimental and theoretical study. *Dalton.Trans.* **2013**, *42*, 11056−11065.
(35) Cao, H. T.; Shan, G. G.; Wen, X. M.; Sun, H. Z.; Su, Z. M.; Zhong, R. L.; Xie, W. F.; Li, P.; Zhu, D. X. An orange iridium(iii) complex with wide-bandwidth in electroluminescence for fabrication

DOI: 10.1021/acs.inorgchem.9b01601
Inorg. Chem. XXXX, XXX, XXX−XXX

of high-quality white organic light-emitting diodes. *J. Mater. Chem. C* **2013**, *1*, 7371−7379.
(36) Cao, H.-T.; Shan, G.-G.; Yin, Y.-M.; Sun, H.-Z.; Wu, Y.; Xie, W.-F.; Su, Z.-M. Modification of iridium(III) complexes for fabrication of high-performance non-doped organic light-emitting diode. *Dyes Pigm.* **2015**, *112*, 8−16.
(37) Mao, H. T.; Zang, C. X.; Shan, G. G.; Sun, H. Z.; Xie, W. F.; Su, Z. M. Achieving High Performances of Nondoped OLEDs Using Carbazole and Diphenylphosphoryl- Functionalized Ir(III) Complexes as Active Components. *Inorg. Chem.* **2017**, *56*, 9979−9987.
(38) Chen, T.-R. Synthesis, structure, and field-effect property of 2-(benzimidazol-2-yl) quinoline. *Mater. Lett.* **2005**, *59*, 1050−1052.
(39) Frisch, M. J.; Trucks, G. W.; Schlegel, H. B.; Scuseria, G. E.; Robb, M. A.; Cheeseman, J. R.; Scalmani, G.; Barone, V.; Mennucci, B.; Petersson, G. A.; Nakatsuji, H.; Caricato, M.; Li, X.; Hratchian, H. P.; Izmaylov, A. F.; Bloino, J.; Zheng, G.; Sonnenberg, J. L.; Hada, M.; Ehara, M.; Toyota, K.; Fukuda, R.; Hasegawa, J.; Ishida, M.; Nakajima, T.; Honda, Y.; Kitao, O.; Nakai, H.; Vreven, T.; Montgomery, J. A., Jr.; Peralta, J. E.; Ogliaro, F.; Bearpark, M.; Heyd, J. J.; Brothers, E.; Kudin, K. N.; Staroverov, V. N.; Keith, T.; Kobayashi, R.; Normand, J.; Raghavachari, K.; Rendell, A.; Burant, J. C.; Iyengar, S. S.; Tomasi, J.; Cossi, M.; Rega, N.; Millam, J. M.; Klene, M.; Knox, J. E.; Cross, J. B.; Bakken, V.; Adamo, C.; Jaramillo, J.; Gomperts, R.; Stratmann, R. E.; Yazyev, O.; Austin, A. J.; Cammi, R.; Pomelli, C.; Ochterski, J. W.; Martin, R. L.; Morokuma, K.; Zakrzewski, V. G.; Voth, G. A.; Salvador, P.; Dannenberg, J. J.; Dapprich, S.; Daniels, A. D.; Farkas, O.; Foresman, J. B.; Ortiz, J. V.; Cioslowski, J.; Fox, D. J. *Gaussian 09, Revision D.01*; Gaussian, Inc.: Wallingford, CT, 2009.
(40) Adamo, C.; Barone, V. Toward reliable density functional methods without adjustable parameters: The PBE0 model. *J. Chem. Phys.* **1999**, *110*, 6158−6170.
(41) Hay, J. P.; Wadt, W. R. Ab initio effective core potentials for molecular calculations. Potentials for K to Au including the outermost core orbitals. *J. Chem. Phys.* **1985**, *82*, 299−310.
(42) Tsuboyama, A.; Iwawaki, H.; Furugori, M.; Mukaide, T.; Kamatani, J.; Igawa, S.; Moriyama, T.; Miura, S.; Takiguchi, T.; Okada, S.; Hoshino, M.; Ueno, K. Homoleptic Cyclometalated Iridium Complexes with Highly Efficient Red Phosphorescence and Application to Organic Light-Emitting Diode. *J. Am. Chem. Soc.* **2003**, *125*, 12971−12979.
(43) Xu, W. J.; Liu, S. J.; Zhao, X. Y.; Sun, S.; Cheng, S.; Ma, T. C.; Sun, H. B.; Zhao, Q.; Huang, W. Cationic iridium(III) complex containing both triarylboron and carbazole moieties as a ratiometric fluoride probe that utilizes a switchable triplet-singlet emission. *Chem. - Eur. J.* **2010**, *16*, 7125−7133.
(44) Xu, W.; Liu, S.; Sun, H.; Zhao, X.; Zhao, Q.; Sun, S.; Cheng, S.; Ma, T.; Zhou, L.; Huang, W. FRET-based probe for fluoride based on a phosphorescent iridium(iii) complex containing triarylboron groups. *J. Mater. Chem.* **2011**, *21*, 7572−7581.
(45) Cummings, S. D.; Eisenberg, R. Tuning the Excited-State Properties of Platinum(II) Diimine Dithiolate Complexes. *J. Am. Chem. Soc.* **1996**, *118*, 1949−1960.
(46) Ho, C.-L.; Wong, W.-Y.; Wang, Q.; Ma, D.; Wang, L.; Lin, Z. A Multifunctional Iridium-Carbazolyl Orange Phosphor for High-Performance Two-Element WOLED Exploiting Exciton-Managed Fluorescence/Phosphorescence. *Adv. Funct. Mater.* **2008**, *18*, 928−937.
(47) Zhao, Q.; Li, F. Y.; Liu, S. J.; Yu, M. X.; Liu, Z. Q.; Yi, T.; Huang, C. H. Highly Selective Phosphorescent Chemosensor for Fluoride Based on an Iridium(III) Complex Containing Arylborane Units. *Inorg. Chem.* **2008**, *47*, 9256−9264.
(48) Ho, C. L.; Wong, W. Y.; Gao, Z. Q.; Chen, C. H.; Cheah, K. W.; Yao, B.; Xie, Z. Y.; Wang, Q.; Ma, D. G.; Wang, L. X.; Yu, X. M.; Kwok, H. S.; Lin, Z. Y. Red-Light-Emitting Iridium Complexes with Hole-Transporting 9-Arylcarbazole Moieties for Electrophosphorescence Efficiency/Color Purity Trade-off Optimization. *Adv. Funct. Mater.* **2008**, *18*, 319−331.
(49) Zhu, Y. C.; Zhou, L.; Li, H. Y.; Xu, Q. L.; Teng, M. Y.; Zheng, Y. X.; Zuo, J. L.; Zhang, H. J.; You, X. Z. Highly efficient green and blue-green phosphorescent OLEDs based on iridium complexes with the tetraphenylimidodiphosphinate ligand. *Adv. Mater.* **2011**, *23*, 4041−4046.
(50) Ho, C. L.; Wang, Q.; Lam, C. S.; Wong, W. Y.; Ma, D.; Wang, L.; Gao, Z. Q.; Chen, C. H.; Cheah, K. W.; Lin, Z. Phosphorescence color tuning by ligand, and substituent effects of multifunctional iridium(III) cyclometalates with 9-arylcarbazole moieties. *Chem. - Asian J.* **2009**, *4*, 89−103.
(51) Wang, Y.; Lu, Y.; Gao, B.; Wang, S.; Ding, J.; Wang, L.; Jing, X.; Wang, F. Self-Host Blue-Emitting Iridium Dendrimer Containing Bipolar Dendrons for Nondoped Electrophosphorescent Devices with Superior High-Brightness Performance. *ACS Appl. Mater. Interfaces* **2016**, *8*, 29600−29607.
(52) Qin, T. S.; Ding, J. Q.; Wang, L. X.; Baumgarten, M.; Zhou, G.; Müllen, K. ADivergent Synthesis of Very Large Polyphenylene Dendrimers with Iridium(III) Cores: Molecular Size Effect on the Performance of Phosphorescent Organic Light-Emitting Diodes. *J. Am. Chem. Soc.* **2009**, *131*, 14329−14336.
(53) Tang, M. C.; Lee, C. H.; Lai, S. L.; Ng, M.; Chan, M. Y.; Yam, V. W. Versatile Design Strategy for Highly Luminescent Vacuum-Evaporable and Solution-Processable Tridentate Gold(III) Complexes with Monoaryl Auxiliary Ligands and Their Applications for Phosphorescent Organic Light Emitting Devices. *J. Am. Chem. Soc.* **2017**, *139*, 9341−9349.
(54) Antoniadis, H.; Abkowitz, M. A.; Hsieh, B. Carrier deep-trapping mobility-lifetime products in poly(p-phenylenevinylene). *Appl. Phys. Lett.* **1994**, *65*, 2030−2032.
(55) Kepler, R. G.; Beeson, P. M.; Jacobs, S. J.; Anderson, R. A.; Sinclair, M. B.; Valencia, V.; Cahill, P. A. Electron and hole mobility in tris(8-hydroxyquinolinolato-N1,O8) aluminum. *Appl. Phys. Lett.* **1995**, *66*, 3618−3620.

DOI: 10.1021/acs.inorgchem.9b01601
Inorg. Chem. XXXX, XXX, XXX−XXX